

# Quantification and qualification by *in-situ* FTIR of species formed on supported-cobalt catalysts during the Fischer-Tropsch reaction

Andrew I. McNab, Alan J. McCue, Davide Dionisi and James A. Anderson\*

Chemical and Materials Engineering Group, School of Engineering, University of Aberdeen,  
Aberdeen, UK, AB24 3UE

Tel: +44 1224 272838, Email\*: [j.anderson@abdn.ac.uk](mailto:j.anderson@abdn.ac.uk)

**Keywords;** FTIR, quantification, Fischer Tropsch, alkyl species, Cobalt catalyst.

## Abstract

*In-situ* FTIR spectroscopy was employed to investigate the location, chain length and quantity of hydrocarbon species adsorbed on supported-cobalt Fischer-Tropsch catalysts. The length of the hydrocarbon units observed was quantified using an appropriately determined absorption coefficient ratio. The individual amounts of CH<sub>2</sub> and CH<sub>3</sub> groups were calculated with absorption coefficients derived specifically for adsorbed hydrocarbon species, unlike previous studies, which employ absorption coefficients derived from liquid phase hydrocarbons. Results show that it is possible for reaction products to re-adsorb from the gas phase onto the support as well as spillover to the support from the active metal cobalt. Qualification and quantification of the chain length of these re-adsorbed species has shown that the support material ( $\gamma$ -alumina) selectively re-adsorbs shorter chain length species from the gas phase with a different functional group to the majority of observable species on a Co/Al<sub>2</sub>O<sub>3</sub> catalyst. Comparison of Co/Al<sub>2</sub>O<sub>3</sub> with Co/SiO<sub>2</sub>, which utilises a more inert support relative to  $\gamma$ -alumina, shows that longer chained species are located on the cobalt metal itself during reaction and can be transported to the  $\gamma$ -alumina support *via* a process of spillover.

## Introduction

The Fischer-Tropsch (FT) synthesis involves the catalytic reaction, at moderate temperatures and pressures, between CO and H<sub>2</sub> (collectively known as syngas) in order to produce liquid transportation fuels as the main products [1]. First discovered in the 1920's [2,3], the process has become more popular in recent decades due the volatile economic nature of the oil and gas industry [4], as well as the need to continue to produce hydrocarbon fuels on

a large scale despite natural oil reserves becoming more difficult to recover. In industry, cobalt or iron are the common choices for the active component of the catalyst due to their high activity and low-cost, respectively [5,6]. Nickel [7] and ruthenium are also known to be active but instead are typically employed as promoters (amongst others such as Au, Cu, Mn, Pd, Pt) for the reaction [8–12]. Various metal oxides ( $\text{Al}_2\text{O}_3$ ,  $\text{SiO}_2$ , and  $\text{TiO}_2$ ) as well as carbon and zeolites have been extensively investigated as supports [13–16].

Despite being in use commercially since around the 1930's, knowledge and understanding of FT synthesis is still somewhat limited and no single proposed reaction mechanism can account for all the experimental data [17,18]. This is, in part, due to the complex product distribution (which varies depending on the catalyst and reaction conditions) that is obtained and includes carbon product chain lengths from 1 to around 40-50. These products also include multiple functionalities such as alkanes, alkenes, branched isomers and numerous oxygenates.

A large proportion of studies have focussed on product analysis for FT synthesis using techniques such as gas chromatography (GC) [19] and mass spectrometry (MS) [20] in order to further understanding of the Anderson-Schulz-Flory (ASF) polymerisation behaviour which occurs [21,22]. Fewer reports however, have studied the catalyst itself during the course of the reaction. Fourier Transform Infrared (FTIR) spectroscopy is an ideal *in-situ* technique to study the catalyst during a reaction such as FT since the recording of spectra is not perturbed by the reaction conditions (i.e. temperature and pressure). FTIR has been utilised to gain qualitative information about the catalyst during FT synthesis, particularly to investigate adsorption sites of CO on supported FT catalysts [23,24]. Previously Jiang *et al.*, employed Diffuse Reflectance Infrared Fourier Transform Spectroscopy (DRIFTS) to study manganese promoted cobalt [25] and iron [26] catalysts and found little or no evidence of adsorbed CO on either promoted or un-promoted cobalt or iron catalysts. This was ascribed to the dissociation of CO on very fine, reduced metallic particles. In contrast, previous work in this laboratory [27] and by other groups [28,29] have observed evidence for the adsorption of CO, using FTIR, on supported-cobalt catalysts under FT conditions.

Some studies have considered the  $\text{C}_x\text{H}_y$  stretching modes observed during the FT reaction. King [30] reported the presence of bands between  $3100\text{-}2700\text{ cm}^{-1}$  for supported Fe and Ru catalysts under FT conditions. For  $\text{Ru/SiO}_2$ , two intense bands were observed at  $2930$  and  $2880\text{ cm}^{-1}$  and were attributed to the asymmetric (asy) and symmetric (sym) stretching

modes of CH<sub>2</sub> species, respectively. On increasing the reaction temperature from 428 to 458 K, these bands decreased in intensity and eventually formed a broad band centred around 2930 cm<sup>-1</sup>, assigned to a mixture of CH<sub>2</sub> and CH<sub>3</sub> groups, and a peak at 3015 cm<sup>-1</sup> associated with gas phase methane. In contrast, spectra of an Fe/SiO<sub>2</sub> catalyst only showed the broad band at 2935 cm<sup>-1</sup>. With increasing temperature, shifts in the relative intensity of bands in the spectra towards lower CH<sub>2</sub>:CH<sub>3</sub> intensities indicate shorter chain length species on the surface of the catalyst, which is consistent with the trend in FT products to decrease chain length with increasing temperature. Schanke *et al.* also reported similar observations for Fe and Ru/SiO<sub>2</sub> catalysts [24]. Prior to the work by King [30], Dalla Betta and Shelef [31], conducted similar experiments with Ru/Al<sub>2</sub>O<sub>3</sub> catalysts and noted that even after the reaction had attained steady state, FTIR bands in the C<sub>x</sub>H<sub>y</sub> region continued to grow, suggesting that these bands are due to reaction products or by-products which are adsorbed on the support. King [30] however, stated that there was insufficient evidence to determine whether these species were solely located on the alumina support. Much more recently, Lorito *et al.* [32] obtained spectra using a Co/Siralox catalyst under a flow of 2:1 H<sub>2</sub>/CO mixture, at typical FT temperatures for Co catalysts (210-230°C). They consider the bands present for CH<sub>2</sub> species to be associated with long chain waxes which accumulated in the catalyst pores.

Few examples exist where the chain length, or quantity of these surface C<sub>x</sub>H<sub>y</sub> species have been determined. Yamasaki *et al.* [33] calculated the average chain length of hydrocarbon species accumulated on a Ru/SiO<sub>2</sub> catalyst during the FT reaction. By calculating the amount of CH<sub>2</sub> and CH<sub>3</sub> units individually (note the authors tabulate quantity in units of volume, cm<sup>3</sup> at s.t.p, not moles), a ratio of the two amounts (CH<sub>2</sub>:CH<sub>3</sub>) resulted in an estimated average chain length of 4 after 3 min time on stream which grew to a value of 20 after 1 h and 30 after 3.5 h. Using a similar method, our group calculated the length of hydrocarbon species adsorbed on Au-promoted and un-promoted Co/Al<sub>2</sub>O<sub>3</sub> catalysts [27,34]. Similar chain lengths of *ca.* 4.4 at steady state were calculated for both catalysts (225°C, 5 bar), however upon increasing the pressure to 10 bar, the average chain length at steady state increased to 5.9 [27]. In these examples [27,33,34], absorption coefficients calculated by Wexler [35] were used to determine the number of CH<sub>2</sub> and CH<sub>3</sub> units. These coefficients were derived using liquid phase hydrocarbons which might be expected to have a higher coefficient value than the species in an adsorbed form as a result of intermolecular interactions, and

therefore their use for adsorbed species may be inappropriate. This issue has been addressed in previous work [36] by attempting to calculate absorption coefficients for the vasy CH<sub>3</sub> and vasy CH<sub>2</sub> (2960 and 2925 cm<sup>-1</sup> respectively) modes for adsorbed hydrocarbon species. While a significant error (*ca.* 20%) was evident for the individual absorption coefficients, it was found that the ratio of these absorption coefficients (across multiple tests, various temperatures and over two different surfaces) have a significantly lower error (*ca.* 6%) and thus, the following expression was formulated to derive the average chain length of the hydrocarbon species using this absorption coefficient ratio:

$$\text{Average } CH_2:CH_3 \text{ ratio of adsorbed species} = \frac{A_{CH_2}/A_{CH_3}}{\varepsilon_{CH_2}:\varepsilon_{CH_3}} \quad \text{Equation 1}$$

where  $A_{CH_x}$  is the integrated absorbance of the band due to a particular stretching mode, and  $\varepsilon_{CH_2}:\varepsilon_{CH_3}$  is the absorption coefficient ratio with a value of 0.36.

This study serves as the first of two parts where the location of the hydrocarbon species detected by FTIR spectroscopy has been investigated to determine where they reside on Co/Al<sub>2</sub>O<sub>3</sub> and Co/SiO<sub>2</sub> catalysts during the FT reaction, i.e., are they found on the support material, metal or both. In addition, the above expression was applied to spectra collected during the course of the reaction in order to monitor the lengths of these species. In the second part, an attempt is made to link these findings to reaction data collected using on-line GC where reaction conditions as well as the active metal used were varied.

## Experimental

### *Catalyst synthesis*

Two 10 wt% loaded Co samples were prepared by wet impregnation of Co(NO<sub>3</sub>)<sub>2</sub>·6H<sub>2</sub>O onto silica and alumina. For the Co/Al<sub>2</sub>O<sub>3</sub> sample,  $\gamma$ -alumina (4.52 g) (Degussa) was wetted (20 ml of water) and stirred before Co(NO<sub>3</sub>)<sub>2</sub>·6H<sub>2</sub>O (2.48 g) (BDH Chemicals Ltd.), which was dissolved in water (2.4 ml), was added drop-wise to the alumina slurry. After further stirring for approximately 40 min, the solution was left to dry slowly **on top of a heating mantle (50°C)** for 48 h. The sample was ground to a fine powder before calcination at 400°C in a flow (50 ml min<sup>-1</sup>) of dry air. The Co/SiO<sub>2</sub> catalyst was prepared by the same method using Co(NO<sub>3</sub>)<sub>2</sub>·6H<sub>2</sub>O (2.47 g) and silica (4.51 g) (Aerosil 200).

### *Catalyst characterisation*

X-ray diffraction (XRD) patterns were collected using a X'Pert Pro diffractometer (Panalytical) with Cu K $\alpha$  monochromatic radiation, using 0.013° steps within a 2 $\theta$  range of

15-60°. Temperature programmed reduction (TPR) analysis was carried out on a TPDRO 1100 Thermo Quest (CE Instruments). Co/Al<sub>2</sub>O<sub>3</sub> (0.047 g) and Co/SiO<sub>2</sub> (0.053 g) samples were placed in a quartz reactor between a quartz wool plug. Reduction was carried out in a flow (20 ml min<sup>-1</sup>) of a 5% H<sub>2</sub>/N<sub>2</sub> mixture, and the sample heated from 40 to 800°C (10°C min<sup>-1</sup>). Gravimetric analysis (to replicate the reduction conditions used in the reaction pre-treatment) was performed with a CI Precision MK2-G5 microbalance attached to a glass vacuum line used for gas manipulation. Powdered samples (*ca.* 40 mg) were loaded into a fritted bucket, before N<sub>2</sub> (25 ml min<sup>-1</sup>) was introduced and the system heated to 350°C using a furnace (Watlow, 120 V). Once the mass had stabilised (2 h period) indicative of dehydration at this temperature, the N<sub>2</sub> was replaced by H<sub>2</sub> (20 ml min<sup>-1</sup>) and continued for 2 h. Data for the mass recording were collected at a sampling rate of 120 min<sup>-1</sup>. The mass difference between the point at which H<sub>2</sub> was introduced and after 2 h was taken as mass loss due to reduction (i.e. mass/moles of oxygen lost) with product water being removed at this temperature. The extent of reduction was calculated by:

$$\% \text{ reduction} = \frac{\text{Moles of oxygen lost}}{\text{Initial moles of oxygen in sample}} \quad \text{Equation 2}$$

Surface area measurements were collected using a Micromeritics Tristar 3000 following a pre-treatment in N<sub>2</sub> at 250°C for 2.5 h. N<sub>2</sub> adsorption isotherms were collected at -196°C between relative pressures of 0.05 and 1. The BET equation was then applied to the resulting data in order to determine surface areas. H<sub>2</sub> chemisorption of catalyst samples was performed using a Micromeritics ASAP 2020-C instrument. Initially samples underwent an *in-situ* reduction (350°C in H<sub>2</sub> for 2 h) before cooling to 35°C. Samples were then exposed to increasing pressures of H<sub>2</sub> (1-400 torr) to produce adsorption isotherms. Monolayer coverage was determined by fitting a Langmuir adsorption isotherm to the collected data assuming dissociative adsorption of H<sub>2</sub>.

#### *Fischer-Tropsch reaction*

Sample powders were pressed into 13 mm diameter self-supporting discs, which were then loaded into a high-temperature, high-pressure FTIR cell (Specac). The consequences of variation in disc preparation in terms of quantification of alkyl species was described in an earlier, related publication [36]. Samples were heated to 350°C in a flow (12 ml min<sup>-1</sup>) of N<sub>2</sub> gas. Once 350°C was attained, the gas flow was switched to H<sub>2</sub> (21 ml min<sup>-1</sup>) for a 2 h reduction period, at which point the samples were then cooled to the reaction temperature

(225°C). Syngas ( $H_2/CO = 2:1$ ) was then introduced, initially at a high flow rate (*ca.* 240 ml  $min^{-1}$ ) until the desired pressure was attained (by means of a back-pressure regulator and taking approximately 5 min to attain the desired pressure). After the pressure was stabilised, a flow rate of 11 ml  $min^{-1}$  (gas hourly space velocity approximately equal to 40000  $h^{-1}$  – NB. gas flow is over a disc, and not through a fixed bed) was set and maintained for the duration of the reaction. Spectra were then collected at various times throughout the reaction using a Perkin Elmer 1700 FTIR Spectrometer at 4  $cm^{-1}$  resolution and an average of 25 spectra. An initial spectrum was collected after the sample pre-treatment, but before the introduction of syngas. This spectrum was subtracted from all subsequently collected spectra during the reaction in order to obtain “difference spectra”. The integrated absorbance for the bands due to the vasy  $CH_3$  and vasy  $CH_2$  modes were determined by deconvolution of the band envelope appearing in the 3100-2700  $cm^{-1}$  region. These derived integrated absorbances were introduced into Equation 1 in order to determine the average chain length of the surface species.

## Results

### *Catalyst characterisation*

Characteristics of the two samples are summarised in Table 1. The surface area of  $Co/Al_2O_3$  and  $Co/SiO_2$  after outgassing at 250°C for 2.5 h was calculated by application of the BET equation and were determined to be 86 and 163  $m^2 g^{-1}$ , respectively (Table 1). Both values are lower than the parent support material (100  $m^2 g^{-1}$  for  $\gamma$ -alumina and 200  $m^2 g^{-1}$  for silica) implying some of the pores may be filled by the cobalt. Figure 1 shows the XRD pattern for both samples. A peak at  $2\theta = 36.9$  is assigned to  $Co_3O_4$  in both cases, however cobalt aluminates ( $CoAl_2O_4$ ) are also known to have a cubic spinel phase like  $Co_3O_4$  with the same diffraction peak positions [37]. Other peaks at  $2\theta = 18.9, 31.4, 44.9,$  and  $59.5$  are also assigned to various other planes of  $Co_3O_4$  and a peak at  $2\theta = 45.7$  present in the  $Co/Al_2O_3$  pattern is indicative of  $\gamma$ -alumina phase [38]. The peak at  $2\theta = 36.9$  was used to estimate the average crystallite size of  $Co_3O_4$  using the Scherrer equation and resulted in crystallite sizes of 21.9 and 29.8 nm for  $Co/Al_2O_3$  and  $Co/SiO_2$ , respectively (Table 1).

Figure 2 displays the TPR profiles for both catalysts. Both samples give two main reduction features at 340°C and a broad feature extending from about 500 to 700°C for  $Co/Al_2O_3$  and at 325 and 360°C for  $Co/SiO_2$ . Jacobs *et al.* [39] explain through combined TPR-XANES/EXAFS

that the first, lower-temperature reduction feature can be assigned to the reduction of  $\text{Co}_3\text{O}_4$  to  $\text{CoO}$ , the presence of the former being consistent with XRD data (Figure 1). The second, higher-temperature reduction feature is strongly influenced by the nature of the support and represents the reduction of  $\text{CoO}$  to  $\text{Co}^0$ . The authors explain that this second reduction feature for  $\text{Co}/\text{SiO}_2$  will occur at lower reduction temperatures relative to alumina-supported samples due to the weaker metal-support interaction, consistent with the profiles shown in Figure 2. As displayed in **Table 1**, the calculated degree of reduction from the TPR analysis is 71 and 100% for  $\text{Co}/\text{Al}_2\text{O}_3$  and  $\text{Co}/\text{SiO}_2$ , respectively after a temperature ramp to  $800^\circ\text{C}$ . Analysis of the two stages for the fully reduced  $\text{Co}/\text{SiO}_2$  sample showed that the first, lower temperature feature accounted for *ca.* 37% of the total uptake. This suggests that the two reduction features may overlap since only a quarter of the total hydrogen uptake is required in the first reduction step ( $\text{Co}_3\text{O}_4$  to  $\text{CoO}$ ) [39].

The gravimetric reduction analysis carried out to replicate the *in-situ* pre-treatment prior to the reaction showed the extent of reduction at  $350^\circ\text{C}$  to be 46 and 79% for  $\text{Co}/\text{Al}_2\text{O}_3$  and  $\text{Co}/\text{SiO}_2$ , respectively. The data obtained from  $\text{H}_2$  chemisorption resulted in uptake values of 12.0 and  $19.8 \mu\text{mol g}^{-1}$  for  $\text{Co}/\text{Al}_2\text{O}_3$  and  $\text{Co}/\text{SiO}_2$  respectively, corresponding to particle sizes of 141 and 85 nm. However, this does not take into account the extent of reduction. Following the procedure of Reuel and Bartholomew [40], the particle size after reduction was calculated from the expression:

$$d = C_1/\%D \quad \text{Equation 3}$$

where  $C_1$  is a constant associated with planar area of a cobalt atom based on the three most common crystallographic planes, the density and molecular weight of cobalt,  $d$  is the particle diameter (nm) and  $\%D$  is the percentage dispersion and is calculated from:

$$\%D = C_2X/Wf \quad \text{Equation 4}$$

where  $C_2$  is a constant associated with cobalt based on the stoichiometry of hydrogen atoms on cobalt surface sites,  $X$  is the  $\text{H}_2$  uptake ( $\mu\text{mol g}^{-1}$ ),  $W$  is the weight percent loading of cobalt, and  $f$  is the fraction of cobalt reduced (values from gravimetric reduction analysis used). Use of this approach resulted in particle sizes of 30.9 and 32.4 nm for  $\text{Co}/\text{Al}_2\text{O}_3$  and  $\text{Co}/\text{SiO}_2$ , respectively (Table 1) which is notably similar, but still larger than the crystallite sizes derived from XRD.

### *Location of surface species*

Figure 3 (a) shows an initial FTIR spectrum collected prior to the reaction and a resulting spectrum (Figure 3 (b)) after 300 min under FT conditions carried out at 225°C, 10 bar using a Co/Al<sub>2</sub>O<sub>3</sub> catalyst. Few features appear in the initial spectrum. A broad band between 3700-3100 cm<sup>-1</sup> for surface hydroxyl species is present as well as peaks at 1577 and 1460 cm<sup>-1</sup> which are attributed to carboxylate species present on the alumina support [41], which are assumed to be the result of carbonation during the calcination stage. After 300 min on stream, numerous other features become obvious, mainly the intense P and R branches of gas phase CO between 2250-2000 cm<sup>-1</sup> (present from the onset). Evidence of carboxylate growth is shown by an increase in intensity of the peaks at 1577 and 1460 cm<sup>-1</sup> as well as the appearance of new bands between 1400-1300 cm<sup>-1</sup> and a shoulder at 1650 cm<sup>-1</sup> which are representative of carboxylate and carbonate type species on the support. A small contribution due to the formation of gas phase CO<sub>2</sub> is shown between 2400-2300 cm<sup>-1</sup>. The remaining bands between 3000-2750 cm<sup>-1</sup> are due CH<sub>x</sub> stretching modes and indicate the extent of formation of hydrocarbon species on the surface of the catalyst. Additional testing was carried out to determine the extent to which spectra collected during the reaction contained contributions due to gas phase hydrocarbons. A disc of the active Co/Al<sub>2</sub>O<sub>3</sub> catalyst was situated in the FTIR cell, but out with the beam-path in order to determine whether gaseous species could be detected. Only a small intensity peak due to gas phase methane (3015 cm<sup>-1</sup>) was observed.

Figure 4 shows difference spectra in the hydrocarbon region (3100-2700 cm<sup>-1</sup>) collected over the duration of the reaction. The two most intense peaks at 2925 and 2860 cm<sup>-1</sup> are attributed to the v<sub>asy</sub> and v<sub>sym</sub> modes of CH<sub>2</sub>, respectively and a shoulder at 2960 cm<sup>-1</sup> is indicative of the v<sub>asy</sub> mode of CH<sub>3</sub>. There is also a small peak present at 3015 cm<sup>-1</sup> due to gas phase methane. The species detected by FTIR which result in the methyl and methylene stretching modes are attributed to adsorbed species which are accumulating on the catalyst surface. There are three possible descriptions to explain the location of these species on the catalyst surface:

1. Hydrocarbon chain growth on active metal sites.
2. Hydrocarbon chain growth on the active metal sites and spillover onto the catalyst support.
3. Hydrocarbon chain growth on the active metal sites followed by desorption and subsequent re-adsorption onto the catalyst support *via* the gas phase.

The term “hydrocarbon species” is employed in its broadest sense to imply a broad range of FT reaction products containing an alkyl chain including oxygenate species. It should be noted that species which are transported to the support may be subjected to further reactions. For example, alcohols have been shown to undergo dehydration on alumina [42]. The transportation of species detected from the active metal sites onto the support was proposed by Dalla Betta and Shelef [31]. In order to ratify if scenario 3 contributes to the resulting spectra, an experiment was carried out, whereby a disc composed of only  $\gamma$ -alumina (calcined at 400°C, 4 h) was positioned in the FTIR beam path, while elsewhere in the cell, a disc of active Co/Al<sub>2</sub>O<sub>3</sub> was located out with the path of the FTIR beam but exposed to the same reactant gas stream and with the sample at reaction temperature. Band growth on the separate disc of  $\gamma$ -alumina should be evident if scenario 3 is taking place. Figure 5 shows the band growth obtained on a separate disc of  $\gamma$ -alumina and thus participation of scenario 3 is confirmed. Similar peak positions as observed for the Co/Al<sub>2</sub>O<sub>3</sub> catalyst for vasy CH<sub>3</sub>, CH<sub>2</sub> and vsym CH<sub>2</sub> at 2960, 2925 and 2860 cm<sup>-1</sup>, respectively, as well as gas phase methane at 3015 cm<sup>-1</sup>. In addition, peaks are present at 2906 cm<sup>-1</sup> and a shoulder at 2885 cm<sup>-1</sup> which are attributed to a methine (CH) stretching mode and the vsym CH<sub>3</sub> mode, respectively. The appearance of a band due to a methine stretching mode where a sample of  $\gamma$ -alumina was present, but which was not observed for Co/Al<sub>2</sub>O<sub>3</sub>, would suggest the presence of a species with a different structure. Other bands observed when adsorption on the alumina sample is monitored support the conclusion of differentiation between species adsorbed on the support and the Co/Al<sub>2</sub>O<sub>3</sub>. These also include bands due to CH stretching mode of aldehydes at *ca.* 2750 cm<sup>-1</sup> and a band assigned to an olefinic =CH<sub>2</sub> stretching mode at 2995 cm<sup>-1</sup>. It should be noted, however, that the intensities of bands when directly monitoring the Co/Al<sub>2</sub>O<sub>3</sub> (Figure 4) are roughly an order of magnitude larger than when monitoring the alumina alone (Figure 5). Therefore the presence of these additional bands may be difficult to detect in the case of the Co/Al<sub>2</sub>O<sub>3</sub>, in part, due to the predominance of other features which, apparently, are not transferred through the gas phase for re-adsorption onto the support.

A comparison of the length of these hydrocarbon chains (determined using Equation 1) generated using either the active sample (Figure 4) or the alumina alone with the active material out with the FTIR beam (Figure 5), is shown in Figure 6. In both cases there is an

initial induction period during the first 3-4 h where the average chain length grows, followed by a decrease in the growth rate followed by a plateau.

The initial chain length is around 4.7 after 5 min for the Co/Al<sub>2</sub>O<sub>3</sub> catalyst, but increases in length to about 7 after 225 min before becoming constant. In contrast, the species detected on the surface of the separate disc of alumina undergo very little progressive growth and are comparably shorter in length to Co/Al<sub>2</sub>O<sub>3</sub>, starting with an average chain length value of 3.1 after 10 min and growing to around 4 units. The amount of adsorbed species was also quantified using the following equation (see reference [34] and references within):

$$\varepsilon = \frac{A.C_d}{n_T.m} \quad \text{Equation 5}$$

where  $\varepsilon$  is the molar absorption coefficient (cm  $\mu\text{mol}^{-1}$ ), A is the integrated absorbance of the particular mode (cm<sup>-1</sup>) – determined by deconvolution of the spectra, C<sub>d</sub> is the area of the sample disc (cm<sup>2</sup>), n<sub>T</sub> is the number of adsorbed species ( $\mu\text{mol g}^{-1}$ ) and m is the initial mass (g) of the sample. C<sub>d</sub> was determined using imaging software, *ImageJ*, which calculates an area based on a user-defined section of a photograph, with known dimensions (in pixels). It should be noted that the absorption coefficients,  $\varepsilon$ , used for vasy CH<sub>3</sub> (3.01 cm  $\mu\text{mol}^{-1}$ ) and vasy CH<sub>2</sub> (1.08 cm  $\mu\text{mol}^{-1}$ ) have a 19 and 20% error attributed to them, respectively [36].

The calculated amounts of adsorbed CH<sub>x</sub> ( $\mu\text{mol g}^{-1}$ ) on Co/Al<sub>2</sub>O<sub>3</sub> and  $\gamma$ -alumina are displayed in Figure 7. For both adsorbents, the individual amounts of CH<sub>2</sub> and CH<sub>3</sub> species continued to grow up to 360 min whereas the average chain length for both adsorbents plateaued after about 225 min (Figure 6). This suggests that between 225 and 360 min more species but of an equivalent chain length are adsorbed.

Analogous experiments were carried out using silica, selected as an example of a more inert support material. Figure 8 shows a selection of spectra collected during reaction for both a Co/SiO<sub>2</sub> catalyst and a disc of silica alone (calcined at 400°C, 4 h) where the Co/Al<sub>2</sub>O<sub>3</sub> was present elsewhere in the cell, out with the path of the FTIR beam. Quantification of the species adsorbed to the Co/SiO<sub>2</sub> catalyst is also presented (Figure 8). The poorer signal-to-noise (S/N) ratio for the spectra arising from the re-adsorbed species on the separate disc of silica, are a consequence of the lower uptake of adsorbate, reducing the confidence levels of the accuracy of deconvolution.

Spectra (Figure 8 top) for Co/SiO<sub>2</sub> (left) and a separate disc of silica (right), show peaks at 2928 and 2860 cm<sup>-1</sup> due to v<sub>asy</sub> and v<sub>sym</sub> CH<sub>2</sub> modes, respectively. A peak due to gas phase methane (3015 cm<sup>-1</sup>) is again evident in the spectra collected for the separate disc of silica, as well as a more obvious shoulder at 2960 cm<sup>-1</sup> due to the v<sub>asy</sub> CH<sub>3</sub> mode than that detected for Co/SiO<sub>2</sub>. The shape of the band envelope using the separate disc of silica would suggest the presence of similar species to those observed on Co/Al<sub>2</sub>O<sub>3</sub> and Co/SiO<sub>2</sub>, unlike that for the case of the separate disc of  $\gamma$ -alumina. The average chain length of the species adsorbed on Co/SiO<sub>2</sub> (Figure 8 bottom left) increases during the first 200 min from an initial value of *ca.* 8 after 50 min (first data point after 50 min due to poor S/N ratio prior to this), before becoming more constant at an approximate value of 9 (2 carbon units longer than the Co/Al<sub>2</sub>O<sub>3</sub> equivalent). Quantification of the amount of CH<sub>3</sub> observed on the Co/SiO<sub>2</sub> catalyst, (26  $\mu\text{mol g}^{-1}$  - Figure 8, bottom right) is considerably less than that observed on Co/Al<sub>2</sub>O<sub>3</sub> (243  $\mu\text{mol g}^{-1}$  - Figure 7).

## Discussion

Characterisation of Co/Al<sub>2</sub>O<sub>3</sub> and Co/SiO<sub>2</sub> catalysts showed the initial oxidic state of cobalt to be Co<sub>3</sub>O<sub>4</sub> using XRD (Figure 1). TPR profiles (Figure 2) suggest a primarily two-step reduction of Co<sub>3</sub>O<sub>4</sub> (i.e., Co<sub>3</sub>O<sub>4</sub>→CoO→Co<sup>0</sup>) takes place, in agreement with the observations of Jacobs *et al.* [39]. However, additional reduction features, which may also be apparent for Co/Al<sub>2</sub>O<sub>3</sub> (Figure 2), include shoulders which are apparent at 400 and 500°C. These features may be explained by the reduction of other cobalt species which may be present after an initial reduction step which may include Co<sup>3+</sup> and Co<sup>2+</sup>. Indeed, Arnoldy and Moulijn [43] reported four individual regions for the reduction of alumina-supported cobalt catalysts; 1) Co<sub>3</sub>O<sub>4</sub> reduction at 327°C, 2) Co<sup>3+</sup> reduction at 477°C, 3) Co<sup>2+</sup> reduction at 627°C and finally 4) reduction of cobalt aluminates at 877°C. Although the reduction temperatures reported by Arnoldy and Moulijn do not match those observed in this study, the authors detail the effect of preparation methods (e.g. calcination temperatures and flow rates) on the reduction temperatures. The Co/SiO<sub>2</sub> catalyst is fully reduced using a temperature programme which reached 800°C, while the Co/Al<sub>2</sub>O<sub>3</sub> catalyst was only 71% reduced (Table 1). These variations are due to the different metal-support interactions associated with alumina and silica, where the latter are relatively weaker, and therefore will result in more

facile reduction [39]. A comparison of the TPR profiles (Figure 2) suggests that the use of a silica support facilitated a much lower reduction temperature for the second reduction step, which decreased from a broad feature for Co/Al<sub>2</sub>O<sub>3</sub> between 500 and 700°C to a sharp feature centred at 360°C for Co/SiO<sub>2</sub>. A much smaller shift for the first reduction feature was evident - 340°C for Co/Al<sub>2</sub>O<sub>3</sub> compared to 325°C for Co/SiO<sub>2</sub>. Based on the amount of hydrogen consumed (37%) for the first reduction feature for the Co/SiO<sub>2</sub> catalyst, it is assumed that an overlap of the reduction steps occurred. Under reduction conditions identical to those used for the FT reaction, again Co/Al<sub>2</sub>O<sub>3</sub> proved more difficult to reduce than Co/SiO<sub>2</sub> (46 versus 79% reduction). Particle size analysis, using data from H<sub>2</sub> chemisorption as well as the gravimetric reduction analysis, resulted in very similar estimated particle sizes for both the alumina and silica-supported catalysts (30.9 and 32.4 nm respectively).

The location of adsorbed hydrocarbons on supported cobalt catalysts during the FT reaction were investigated by *in-situ* FTIR. Analysis of a Co/Al<sub>2</sub>O<sub>3</sub> catalyst, produced spectra (Figure 4) where CH<sub>2</sub> (v<sub>asy</sub> and v<sub>sym</sub> modes at 2928 and 2860 cm<sup>-1</sup>, respectively) appeared to be the dominant fragments in the spectra collected in the range 3100-2700 cm<sup>-1</sup>. Also present was the band due to the v<sub>asy</sub> mode of CH<sub>3</sub> (2960 cm<sup>-1</sup>). These are predominantly indicative of hydrocarbon reaction products which have adsorbed to the catalyst, or more specifically to the support, as reported by Dalla Betta and Shelef [31] when investigating the FT reaction using *in-situ* IR on a Ru/Al<sub>2</sub>O<sub>3</sub> catalyst. King [30] stated that there was insufficient evidence to confirm that the hydrocarbons were only adsorbed to the support and that they could in fact be present on the metal as well. In this study, the use of the “separate disc” experiment and the use of alternative supports have allowed further insight into this issue. Band growth occurred over the duration of a reaction when a disc of the support material,  $\gamma$ -alumina, was present in the path of the FTIR beam (Figure 5), while elsewhere in the cell, FT active Co/Al<sub>2</sub>O<sub>3</sub> catalyst was present. Band growth on the separate disc of alumina would only happen, if some of the reaction products re-adsorb to the support from the gas phase, hence scenario 3 (as referenced earlier) is proven. The spectra collected using the disc of  $\gamma$ -alumina resulted in a different band envelope in comparison to the Co/Al<sub>2</sub>O<sub>3</sub> catalyst. The presence of bands due to methine (2906 cm<sup>-1</sup>), bands due to CH stretching mode of aldehydes (*ca.* 2750 cm<sup>-1</sup>) and olefinic =CH<sub>2</sub> stretching mode (2995 cm<sup>-1</sup>), which are not present (or at least in any significant, observable amount relative to the intensities of other

bands which are present) on the Co/Al<sub>2</sub>O<sub>3</sub> sample, would suggest a different hydrocarbon species has re-adsorbed on the support material. With evidence of re-adsorption of reaction products to the support from the gas phase, those species should indeed be present on the Co/Al<sub>2</sub>O<sub>3</sub> sample. However, the shapes of the band envelope in spectra for the Co/Al<sub>2</sub>O<sub>3</sub> sample are vastly different to that on the separate disc of  $\gamma$ -alumina. Therefore it can be said that the spectra obtained for the Co/Al<sub>2</sub>O<sub>3</sub> must be a combination of reaction products which have re-adsorbed on the support from the gas phase as well as hydrocarbons which reside on the active metal and/or species which are transported to the support by other means, i.e. spillover. Table 2 summaries the average hydrocarbon chain length present on the various adsorbents tested using Equation 1 for the initial and final data points. The average length of adsorbed products on the Co/Al<sub>2</sub>O<sub>3</sub> catalyst was shown to grow by 2.6 carbon units over the duration of the reaction, with a maximum value of 7.3 reached after 225 min time on stream. In comparison, very little growth was shown for the separate disc of  $\gamma$ -alumina, with a maximum value of 3.9 attained which initially began at 3.1. These re-adsorbed products are therefore suggested to be selectively adsorbed, shorter chained species which differ in structure compared to the majority of the species observed on the Co/Al<sub>2</sub>O<sub>3</sub> catalyst. Since, as discussed, the spectra obtained using a Co/Al<sub>2</sub>O<sub>3</sub> catalyst are a combination of re-adsorbed products and other hydrocarbons located elsewhere, the calculated average value for the chain length for Co/Al<sub>2</sub>O<sub>3</sub> must be reduced as a consequence of the presence of these shorter chained products re-adsorbed on the support (i.e. there are other longer chained hydrocarbon fragments on the Co component). When analogous tests were carried out using a separate disc of silica, re-adsorption had occurred, but in a quantity too insignificant to quantify. Therefore, with little re-adsorption to the silica support, it is suggested that the chain lengths determined using the Co/SiO<sub>2</sub> catalyst are more indicative of the hydrocarbons which reside on the active cobalt metal and would be expected to be longer than those observed on the Co/Al<sub>2</sub>O<sub>3</sub> catalyst. Indeed, for the Co/SiO<sub>2</sub> catalyst, the calculated average chain length reached a maximum of 9.3 as compared to 7.3 calculated for Co/Al<sub>2</sub>O<sub>3</sub>.

The number of moles of CH<sub>2</sub> and CH<sub>3</sub> adsorbed on Co/Al<sub>2</sub>O<sub>3</sub> and the  $\gamma$ -alumina support as determined by use of Equation 5 are shown (Figure 7). If it is assumed that a hydrocarbon chain attached to the surface of the catalyst terminates in a CH<sub>3</sub> group, then the number of CH<sub>3</sub> fragments would equal the total number of adsorbed hydrocarbon fragments (this

assumes the absence of branched chained products). Therefore, the data (Table 2) would suggest that there is approximately 5-fold more individual hydrocarbon chains adsorbed on the Co/Al<sub>2</sub>O<sub>3</sub> catalyst compared to the separate disc of  $\gamma$ -alumina after 360 min (243  $\mu\text{mol g}^{-1}$  of CH<sub>3</sub> on Co/Al<sub>2</sub>O<sub>3</sub> and 45  $\mu\text{mol g}^{-1}$  of CH<sub>3</sub> on  $\gamma$ -alumina). The percentage of the carbon in the feed stream which is retained on the surface of the Co/Al<sub>2</sub>O<sub>3</sub> catalyst can be calculated based on these estimations. If the average CH<sub>2</sub>:CH<sub>3</sub> ratio is 7 after 360 min, which would indicate an actual chain length of 8, then the total number of moles of carbon can be determined and compared to the total amount of carbon (in the form of CO) introduced to the reactor. It is estimated that 0.01% of the total inlet carbon is retained on the Co/Al<sub>2</sub>O<sub>3</sub> catalyst surface.

Surface coverages may be calculated if it is assumed that the adsorption sites for the hydrocarbon fragments on the support are hydroxyl groups. Digne *et al.* [44] report a range of surface hydroxyl group densities from 12.0 at 177°C to 4.9 OH nm<sup>-2</sup> at 607°C for standard  $\gamma$ -alumina. Having calcined the Co/Al<sub>2</sub>O<sub>3</sub> catalyst at 400°C (the highest temperature treatment applied to the catalyst), a hydroxyl concentration of 8.3 OH nm<sup>-2</sup> is suggested for the support material. However, it should be noted that this value is not definitive due to, for example, water being produced during the reduction of the catalyst (or the FT reaction itself) which may alter this value. Based on this hydroxyl group concentration, the coverage,  $\theta$ , was calculated using:

$$\theta = \frac{\text{No. of CH}_3 \text{ groups}}{\text{No. of OH surface sites}} \quad \text{Equation 6}$$

The extent of coverage on the  $\gamma$ -alumina support due to re-adsorption of gaseous reaction products was determined to be  $\theta = 0.03$  and  $0.05$  after 360 and 1440 min, respectively. In comparison, the coverage for Co/Al<sub>2</sub>O<sub>3</sub> was found to be considerably higher at  $\theta = 0.21$  after 360 min and  $\theta = 0.42$  after 1440 min. Applying the H<sub>2</sub> chemisorption data to the Co/Al<sub>2</sub>O<sub>3</sub> catalyst used, the number of available surface Co atoms is determined to be  $1.08 \times 10^{17}$ . In comparison to the amount of CH<sub>3</sub> groups calculated after 360 min for Co/Al<sub>2</sub>O<sub>3</sub>, the number of exposed Co atoms is 20 times less and 41 times less after 1440 min than the number of hydrocarbon fragments. It should be stated that this assumes that each available Co atom can accommodate a hydrocarbon chain which may not be possible due to, for example,

steric hindrance. When considering this as well as comparing the coverages observed on the  $\gamma$ -alumina support and the Co/Al<sub>2</sub>O<sub>3</sub> catalysts, it would suggest that a considerable amount of species must spillover to the support.

To consider spillover from active metal cobalt particles to the support for a Co/Al<sub>2</sub>O<sub>3</sub> catalyst, the radial distance from a cobalt particle that the total number of hydrocarbons (based on the number of CH<sub>3</sub> units present) must diffuse across in order to attain a 1:1 ratio of CH<sub>3</sub> : OH for the coverages calculated and a theoretical full coverage, i.e.  $\theta = 1$ , is shown in Figure 9. The data shown (Figure 9) was determined by calculating the number of OH groups in a circular area, excluding the area of the cobalt particle, and then scaled up to apply for the catalyst as a whole based on the total number of cobalt particles. By comparing with the estimated number of CH<sub>3</sub> groups present at various reaction times, the maximum distance that a hydrocarbon species would have to diffuse across the surface in order to account for a 1:1 ratio of CH<sub>3</sub> : OH can be calculated. Assuming an OH concentration of 8.3 nm<sup>-2</sup> after 360 min (21% coverage), a radius of 80 nm from the centre (or 64.5 nm from the edge) of the cobalt particle would be required in order to attain a 1:1 ratio. After 1440 min (42% coverage), 112.5 nm from the centre (or 97 nm from the edge) of the cobalt particle would be required and at complete surface coverage, 175 nm from the centre (or 159.5 nm from the edge) of the cobalt particle would attain a 1:1 ratio. Additional OH concentrations have also been modelled (4.9 and 12.0 OH nm<sup>-2</sup> - Figure 9). It is evident that at lower OH concentrations, migration of the species appears to occur over a large distance since the adsorption sites are spread further apart, and conversely at higher OH concentrations, the species do not have to migrate as far to obtain a 1:1 CH<sub>3</sub> : OH ratio. This model makes the assumptions that none of the hydrocarbon chains contain any branches which would alter the CH<sub>3</sub> : OH ratio, and that all of the species are indeed spilled over to the support (which has already been shown not to be the case due to re-adsorption from the gas phase). As stated, after 360 min (21% coverage), a radius of 80 nm from the centre of the cobalt particle would suffice for a 1:1 CH<sub>3</sub> : OH ratio for an OH concentration of 8.3 OH nm<sup>-2</sup>. This appears to be a large distance to diffuse across the surface, however, giving that even after only 360 min, the amount of CH<sub>3</sub> (243  $\mu$ mol g<sup>-1</sup> - Table 2) outnumbers the sum of the available Co sites (12  $\mu$ mol g<sup>-1</sup> - Table 1) and the quantity of re-adsorbed species from the gas phase (45  $\mu$ mol g<sup>-1</sup> - Table 2), a scenario by which the hydrocarbons migrate large distances across the support should be considered. In a review by Conner and Falconer

[45], the migration of spilt over species is discussed and although the transfer of species over large distances is debated, examples are known where spill-over hydrogen has been shown to travel over millimetres or even centimetres on silica surfaces [46]. Conner and Falconer [45] describe a “bucket brigade” like transport whereby hydrogen diffusion across an oxide surface is facilitated by surface hydroxyl groups.

It should also be noted that, the length of adsorbed hydrocarbons on FT catalysts have been previously calculated [27,33] utilising absorption coefficients [35] which were determined from liquid phase hydrocarbon compounds. In separate tests [27], an initial CH<sub>2</sub>:CH<sub>3</sub> ratio of 2.9 was found, which rose to a constant value of 5.9 for a 10 wt% Co/Al<sub>2</sub>O<sub>3</sub> catalyst under analogous conditions (225°C, 10 bar, H<sub>2</sub>/CO = 2:1), using Wexler’s [35] coefficients. These chain lengths are shorter in comparison to the initial (4.9) and final (7.3) values determined in this study. This difference is attributed to the use of liquid phase derived absorption coefficients (where a larger vibrational response per mole would be expected relative to the adsorbed form) being applied to adsorbed species.

## Conclusions

*In-situ* FTIR spectroscopy was implemented to investigate the location, length and amount of hydrocarbon species detected at the surface of supported-cobalt catalysts during the FT reaction. The use of the “separate disc” experiment showed it was possible for species to be transported to the  $\gamma$ -alumina support of a Co/Al<sub>2</sub>O<sub>3</sub> catalyst by re-adsorption of products from the gas phase. A qualitative comparison of the species present in spectra collected from the Co/Al<sub>2</sub>O<sub>3</sub> and the separate disc of  $\gamma$ -alumina suggests that the re-adsorbed species are of a differing structure to the majority of species observed for Co/Al<sub>2</sub>O<sub>3</sub>. In addition, the average length of the re-adsorbed species was determined to be significantly shorter than those observed for Co/Al<sub>2</sub>O<sub>3</sub>. Quantification of hydrocarbons observed on a Co/SiO<sub>2</sub> catalyst, where silica acts as a much more inert support, suggested that longer chained species reside on the cobalt metal itself. Through quantifying the individual hydrocarbon chains, it was evident that not all of the observed hydrocarbons remain on the available cobalt sites and that transfer and re-adsorption of the products to the  $\gamma$ -alumina support would likely only account for a small fraction of the total number of hydrocarbon species. The possibility of hydrocarbon chains spilling over to the support *via* surface diffusion from

the cobalt metal was postulated, and shown to occur, possibly over large distances. Further work is to be conducted where any link between the hydrocarbon species observed by FTIR and reaction products is to be investigated.

## Acknowledgements

## References

- [1] H. Schulz, Short history and present trends of Fischer–Tropsch synthesis, *Appl. Catal. A Gen.* 186 (1999) 3–12. doi:10.1016/S0926-860X(99)00160-X.
- [2] F. Fischer, H. Tropsch, Uber die direkte synthese von Erdol-Kohlenwasserstoffen bei gewonlichem druck, *Chem. Ber.* 59 (1926) 830–831.
- [3] F. Fischer, H. Tropsch, Uber die direkte synthese von Erdol-kohlenwasserstoffen bei gewonlichem druck, *Chem. Ber.* 59 (1926) 832–836.
- [4] H.C. Mantripragada, E.S. Rubin, Techno-economic evaluation of coal-to-liquids (CTL) plants with carbon capture and sequestration, *Energy Policy.* 39 (2011) 2808–2816. doi:10.1016/j.enpol.2011.02.053.
- [5] E. de Smit, B.M. Weckhuysen, The renaissance of iron-based Fischer-Tropsch synthesis: on the multifaceted catalyst deactivation behaviour., *Chem. Soc. Rev.* 37 (2008) 2758–81. doi:10.1039/b805427d.
- [6] B.Y.F. Morales, B.M. Weckhuysen, Promotion Effects in Co-based Fischer – Tropsch Catalysis, *Catalysis.* 19 (2006) 1–40.
- [7] B.C. Enger, A. Holmen, Nickel and Fischer-Tropsch Synthesis, *Catal. Rev. Sci. Eng.* 54 (2012) 437–488. doi:10.1080/01614940.2012.670088.
- [8] K. Jalama, N.J. Coville, H. Xiong, D. Hildebrandt, D. Glasser, S. Taylor, A. Carley, J. a. Anderson, G.J. Hutchings, A comparison of Au/Co/Al<sub>2</sub>O<sub>3</sub> and Au/Co/SiO<sub>2</sub> catalysts in the Fischer–Tropsch reaction, *Appl. Catal. A Gen.* 395 (2011) 1–9. doi:10.1016/j.apcata.2011.01.002.
- [9] J. Wang, P. a. Chernavskii, A.Y. Khodakov, Y. Wang, Structure and catalytic performance of alumina-supported copper–cobalt catalysts for carbon monoxide hydrogenation, *J. Catal.* 286 (2012) 51–61. doi:10.1016/j.jcat.2011.10.012.
- [10] A. Dinse, M. Aigner, M. Ulbrich, G.R. Johnson, A.T. Bell, Effects of Mn promotion on the activity and selectivity of Co/SiO<sub>2</sub> for Fischer–Tropsch Synthesis, *J. Catal.* 288 (2012) 104–114. doi:10.1016/j.jcat.2012.01.008.

- [11] M. Luo, R.O. Brien, B.H. Davis, Effect of palladium on iron Fischer – Tropsch synthesis catalysts, *Catal. Letters*. 98 (2004) 17–22.
- [12] H. Karaca, O. V. Safonova, S. Chambrey, P. Fongarland, P. Roussel, A. Griboval-Constant, M. Lacroix, A.Y. Khodakov, Structure and catalytic performance of Pt-promoted alumina-supported cobalt catalysts under realistic conditions of Fischer–Tropsch synthesis, *J. Catal.* 277 (2011) 14–26. doi:10.1016/j.jcat.2010.10.007.
- [13] S. Storsater, B. Totdal, J. Walmsley, B. Tanem, A. Holmen, Characterization of alumina-, silica-, and titania-supported cobalt Fischer–Tropsch catalysts, *J. Catal.* 236 (2005) 139–152. doi:10.1016/j.jcat.2005.09.021.
- [14] E. Rytter, A. Holmen, On the support in cobalt Fischer – Tropsch synthesis — Emphasis on alumina and aluminates, *Catal. Today*. 275 (2016) 11–19. doi:10.1016/j.cattod.2015.11.042.
- [15] S. Karimi, A. Tavasoli, Y. Mortazavi, A. Karimi, Cobalt supported on Graphene – A promising novel Fischer – Tropsch synthesis catalyst, *Appl. Catal. A, Gen.* 499 (2015) 188–196. doi:10.1016/j.apcata.2015.04.024.
- [16] Y. Liu, J. Luo, M. Girleanu, O. Ersen, C. Pham-Huu, C. Meny, Efficient hierarchically structured composites containing cobalt catalyst for clean synthetic fuel production from Fischer–Tropsch synthesis, *J. Catal.* 318 (2014) 179–192. doi:10.1016/j.jcat.2014.08.006.
- [17] B.H. Davis, Fischer–Tropsch synthesis: current mechanism and futuristic needs, *Fuel Process. Technol.* 71 (2001) 157–166. doi:10.1016/S0378-3820(01)00144-8.
- [18] M. Ojeda, R. Nabar, A.U. Nilekar, A. Ishikawa, M. Mavrikakis, E. Iglesia, CO activation pathways and the mechanism of Fischer–Tropsch synthesis, *J. Catal.* 272 (2010) 287–297. doi:10.1016/j.jcat.2010.04.012.
- [19] Y. Yao, X. Liu, D. Hildebrandt, D. Glasser, Fischer-Tropsch Synthesis Using H<sub>2</sub>/CO/CO<sub>2</sub> Syngas Mixtures over an Iron Catalyst, *Ind. Eng. Chem. Res.* 50 (2011) 11002–11012.
- [20] K. Seomoon, On-line GC and GC–MS analyses of the Fischer–Tropsch products synthesized using ferrihydrite catalyst, *J. Ind. Eng. Chem.* 19 (2013) 2108–2114. doi:10.1016/j.jiec.2013.05.022.
- [21] J. Gao, B. Wu, L. Zhou, Y. Yang, X. Hao, J. Xu, Y. Xu, Y. Li, Irregularities in Product Distribution of Fischer–Tropsch Synthesis Due to Experimental Artifact, *Ind. Eng. Chem. Res.* 51 (2012) 11618–11628. doi:10.1021/ie201671g.

- [22] I. Puskas, R.. Hurlbut, Comments about the causes of deviations from the Anderson–Schulz–Flory distribution of the Fischer–Tropsch reaction products, *Catal. Today*. 84 (2003) 99–109. doi:10.1016/S0920-5861(03)00305-5.
- [23] M.M. McClory, R.D. Gonzalez, The Role of Alkali Metals as Promoters in the methanation Reaction : An in Situ Study, *J. Catal.* 89 (1984) 392–403.
- [24] D. Schanke, G.R. Fredriksen, E.A. Blekkan, A. Holmen, CO hydrogenation on SiO<sub>2</sub>-supported Fe and Ru catalysts studied by in situ IR spectroscopy, *Catal. Today*. 9 (1991) 69–76.
- [25] M. Jiang, N. Koizumi, T. Ozaki, M. Yamada, Adsorption properties of cobalt and cobalt-manganese catalysts studied by in situ diffuse reflectance FTIR using CO and CO+H<sub>2</sub> as probes, *Appl. Catal. A Gen.* 209 (2001) 59–70. doi:10.1016/S0926-860X(00)00755-9.
- [26] M. Jiang, N. Koizumi, M. Yamada, Adsorption Properties of Iron and Iron - Manganese Catalysts Investigated by in-situ Diffuse Reflectance FTIR Spectroscopy, *J. Phys. Chem. B*. 104 (2000) 7636–7643.
- [27] A.J. McCue, J. Aponaviciute, R.P.K. Wells, J.A. Anderson, Gold modified cobalt-based Fischer-Tropsch catalysts for conversion of synthesis gas to liquid fuels, *Front. Chem. Sci. Eng.* 7 (2013) 262–269. doi:10.1007/s11705-013-1334-5.
- [28] J. Couble, D. Bianchi, Experimental Microkinetic Approach of the Surface Reconstruction of Cobalt Particles in Relationship with the CO / H<sub>2</sub> Reaction on a Reduced 10 % Co / Al<sub>2</sub>O<sub>3</sub> Catalyst, *J. Phys. Chem. C*. 117 (2013) 14544–14557.
- [29] A. Paredes-Nunez, D. Lorito, N. Guilhaume, C. Mirodatos, Y. Schuurman, F.C. Meunier, Nature and reactivity of the surface species observed over a supported cobalt catalyst under CO/H<sub>2</sub> mixtures, *Catal. Today*. 242 (2015) 178–183. doi:10.1016/j.cattod.2014.04.033.
- [30] D.L. King, An in situ infrared study of CO hydrogenation over silica and alumina-supported ruthenium and silica-supported iron, *J. Catal.* 61 (1980) 77–86.
- [31] R.A. Dalla Betta, M. Shelef, Heterogeneous Methanation : In Situ Infrared Spectroscopic Study of Ru/Al<sub>2</sub>O<sub>3</sub> during the Hydrogenation of CO, *J. Catal.* 48 (1977) 111–119.
- [32] D. Lorito, a. Paredes-Nunez, C. Mirodatos, Y. Schuurman, F.C. Meunier, Determination of formate decomposition rates and relation to product formation

- during CO hydrogenation over supported cobalt, *Catal. Today*. 259 (2016) 192–196. doi:10.1016/j.cattod.2015.06.027.
- [33] H. Yamasaki, Y. Kobori, S. Naito, T. Onishi, K. Tamaru, Infrared Study of the Reaction of H<sub>2</sub>+CO on a Ru/SiO<sub>2</sub> Catalyst, *J. Chem. Soc., Faraday Trans. 1*. 77 (1981) 2913–2925.
- [34] A.J. McCue, G.A. Mutch, A.I. McNab, S. Campbell, J.A. Anderson, Quantitative determination of surface species and adsorption sites using Infrared spectroscopy, *Catal. Today*. (2015). doi:10.1016/j.cattod.2015.03.039.
- [35] A.S. Wexler, Infrared determination of structural units in organic compounds by integrated intensity measurements : Alkanes , alkenes and monosubstituted alkyl benzenes, *Spectrochem. Acta*. 21 (1965) 1725–1742.
- [36] A.I. McNab, T. Heinze, A.J. McCue, D. Dionisi, J.A. Anderson, Quantification of hydrocarbon species on surfaces by combined microbalance-FTIR, *Spectrochim. Acta Part A Mol. Biomol. Spectrosc.* 181 (2017) 65–72. doi:10.1016/j.saa.2017.03.030.
- [37] K.N. Papageridis, G. Siakavelas, N.D. Charisiou, D.G. Avraam, L. Tzounis, K. Kousi, M.A. Goula, Comparative study of Ni, Co, Cu supported on  $\gamma$ -alumina catalysts for hydrogen production via the glycerol steam reforming reaction, *Fuel Process. Technol.* 152 (2016) 156–175. doi:10.1016/j.fuproc.2016.06.024.
- [38] L. Ji, J. Lin, H.C. Zeng, Metal-support interactions in Co/Al<sub>2</sub>O<sub>3</sub> catalysts: A comparative study on reactivity of support, *J. Phys. Chem. B*. 104 (2000) 1783–1790. doi:10.1021/Jp993400l.
- [39] G. Jacobs, Y. Ji, B.H. Davis, D. Cronauer, A.J. Kropf, C.L. Marshall, Fischer–Tropsch synthesis: Temperature programmed EXAFS/XANES investigation of the influence of support type, cobalt loading, and noble metal promoter addition to the reduction behavior of cobalt oxide particles, *Appl. Catal. A Gen.* 333 (2007) 177–191. doi:10.1016/j.apcata.2007.07.027.
- [40] R.C. Reuel, C.H. Bartholomew, The stoichiometries of H<sub>2</sub> and CO adsorptions on cobalt: Effects of support and preparation, *J. Catal.* 85 (1984) 63–77. doi:10.1016/0021-9517(84)90110-6.
- [41] J. Datka, Z. Sarbak, R.P. Eischens, Infrared Study of Coke on Alumina and Zeolite, *J. Catal.* 145 (1994) 544–550. doi:10.1006/jcat.1994.1065.
- [42] E.C. DeCanio, V.P. Nero, J.W. Bruno, Identification of Alcohol Adsorption Sites on  $\gamma$ -Alumina, *J. Catal.* 135 (1992) 444–457.

- [43] P. Arnoldy, J.A. Moulijn, Temperature-Programmed Reduction of CoO/Al<sub>2</sub>O<sub>3</sub> Catalysts, *J. Catal.* 93 (1985) 38–54.
- [44] M. Digne, P. Sautet, P. Raybaud, P. Euzen, H. Toulhoat, Hydroxyl Groups on  $\gamma$  - Alumina Surfaces : A DFT Study, *J. Catal.* 211 (2002) 1–5. doi:10.1006/jcat.2002.3741.
- [45] W.C. Conner, J.L. Falconer, Spillover in Heterogeneous Catalysis, *Chem. Rev.* 95 (1995) 759–788. doi:10.1021/cr00035a014.
- [46] J.F.. Cevallos-Candau, W.C. Conner, The spillover of hydrogen onto silica. IV. The use of scanning FTIR to follow spillover from a point source, *J. Catal.* 106 (1987) 378–385. doi:10.1016/0021-9517(87)90249-1.

## Tables

**Table 1: Characteristics of Co/Al<sub>2</sub>O<sub>3</sub> and Co/SiO<sub>2</sub>.**

Analysis	Sample	
	Co/Al <sub>2</sub> O <sub>3</sub>	Co/SiO <sub>2</sub>
Surface area (m <sup>2</sup> g <sup>-1</sup> ) <sup>a</sup>	86	163
XRD crystallite size (nm) <sup>b</sup>	21.9	29.8
TPR analysis (%) <sup>c</sup>	71	100
Gravimetric reduction (%) <sup>d</sup>	46	79
H <sub>2</sub> uptake (μmol g <sup>-1</sup> ) <sup>e</sup>	12.0	19.8
Particle size (nm) <sup>f</sup>	30.9	32.4

<sup>a</sup> Determined for N<sub>2</sub> adsorption by application of the BET equation.

<sup>b</sup> Calculated using Scherrer equation applied to peak at 2θ = 36.9 .

<sup>c</sup> Based on integrated area of TPR patterns converted to an amount of H<sub>2</sub> consumed, as a percentage of the theoretical total H<sub>2</sub> uptake possible for the complete reduction of cobalt present.

<sup>d</sup> Calculated with Equation 2 based on mass loss observed in gravimetric analysis, as a percentage of the theoretical initial oxygen content.

<sup>e</sup> Based on H<sub>2</sub> chemisorption isotherms collected at 35°C.

<sup>f</sup> From particle size Equations 3 and 4 [40] taking into account gravimetric reduction analysis and H<sub>2</sub> uptake.

**Table 2: Summary of calculated values for various adsorbents.**

Adsorbent	Average chain length after (X min)	Average chain length after 360 min	CH <sub>3</sub> adsorbed after 360 min (μmol g <sup>-1</sup> )	CH <sub>3</sub> adsorbed after 1440 min (μmol g <sup>-1</sup> )
Co/Al <sub>2</sub> O <sub>3</sub>	4.7 (5 min)	7.3	243	495
Al <sub>2</sub> O <sub>3</sub>	3.1 (10 min)	3.9	45	73
Co/SiO <sub>2</sub>	7.9 (50 min)	9.3	26	36

## Figures

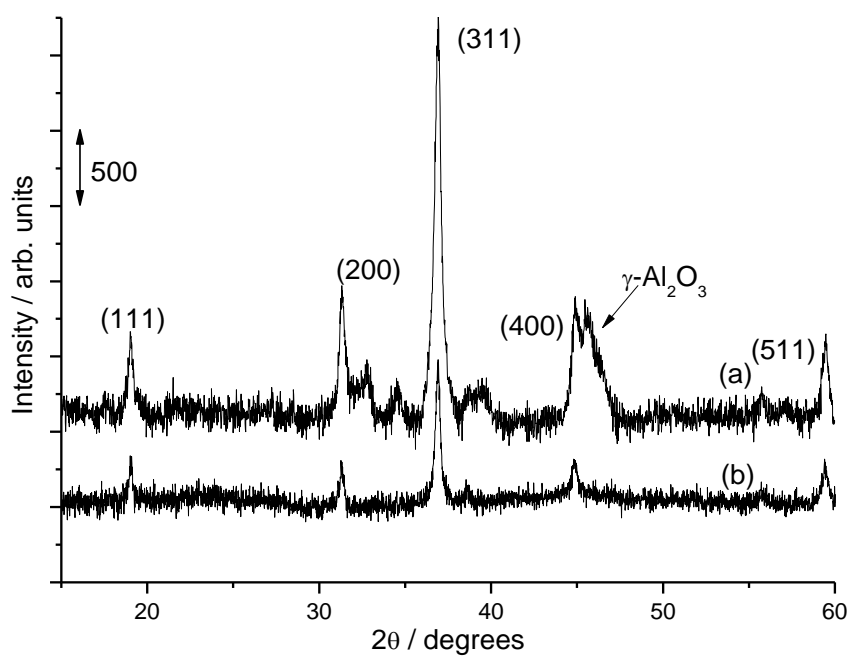


Figure 1: XRD pattern of (a)  $\text{Co}/\text{Al}_2\text{O}_3$  and (b)  $\text{Co}/\text{SiO}_2$ .

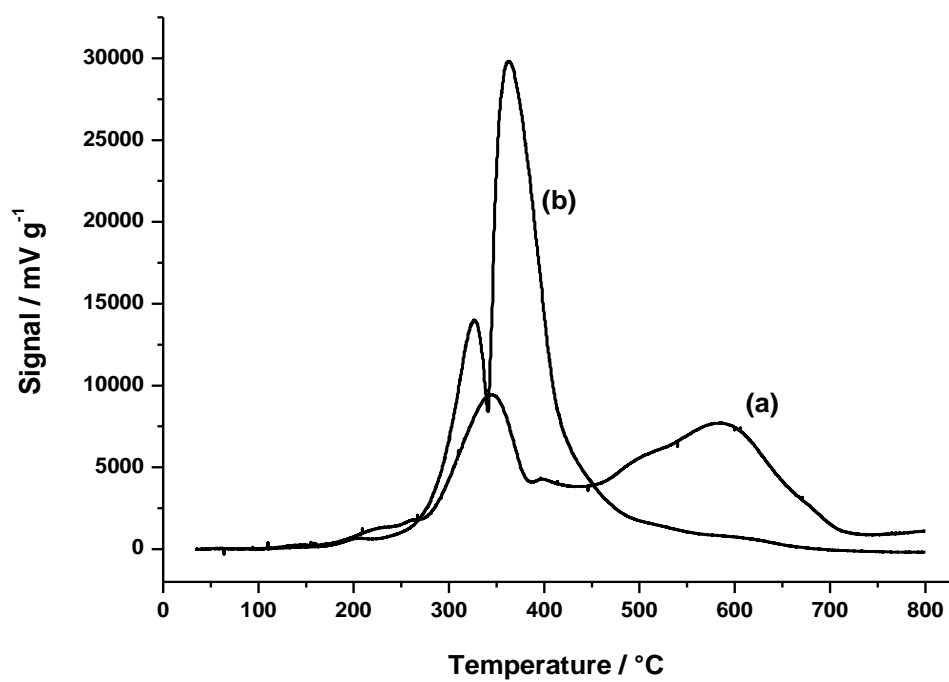
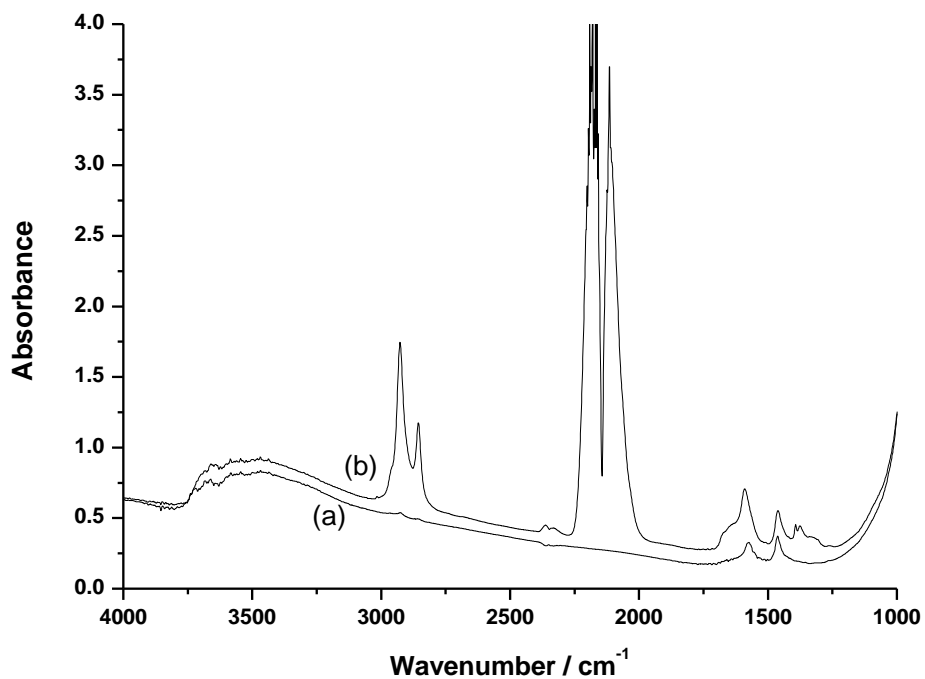
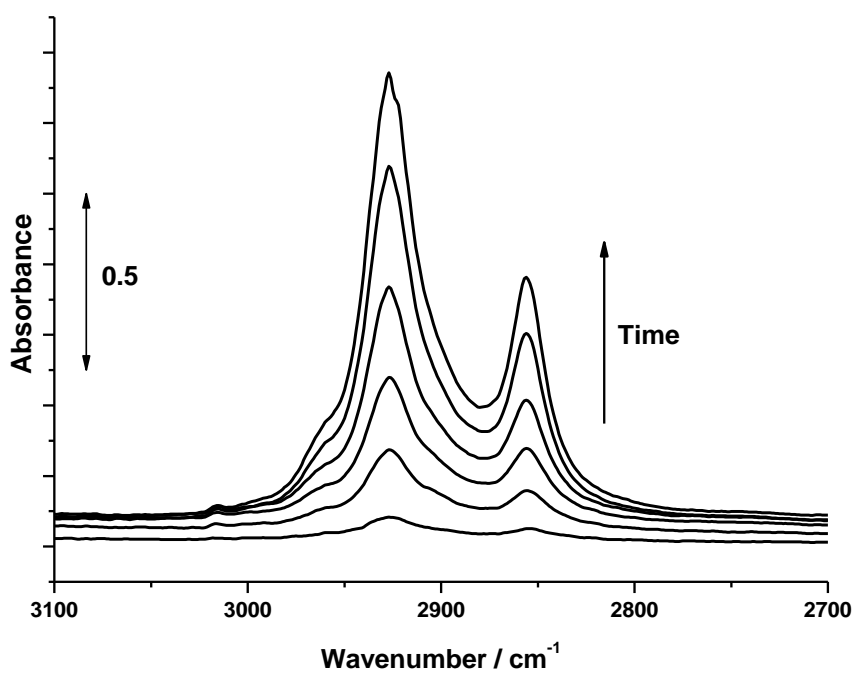


Figure 2: TPR profiles for (a) 10 wt%  $\text{Co}/\text{Al}_2\text{O}_3$  and (b) 10 wt%  $\text{Co}/\text{SiO}_2$ .



**Figure 3:** FTIR spectra at t=0 min (a) and t=300 min (b) for a Co/Al<sub>2</sub>O<sub>3</sub> catalysts under FT conditions (225°C, 10 bar, H<sub>2</sub>/CO = 2:1).



**Figure 4:** Selection of FTIR difference spectra for hydrocarbon region collected at 5, 25 60, 120, 240 and 360 min time on stream for a Co/Al<sub>2</sub>O<sub>3</sub> catalyst under FT conditions (225°C, 10 bar, H<sub>2</sub>/CO = 2:1).

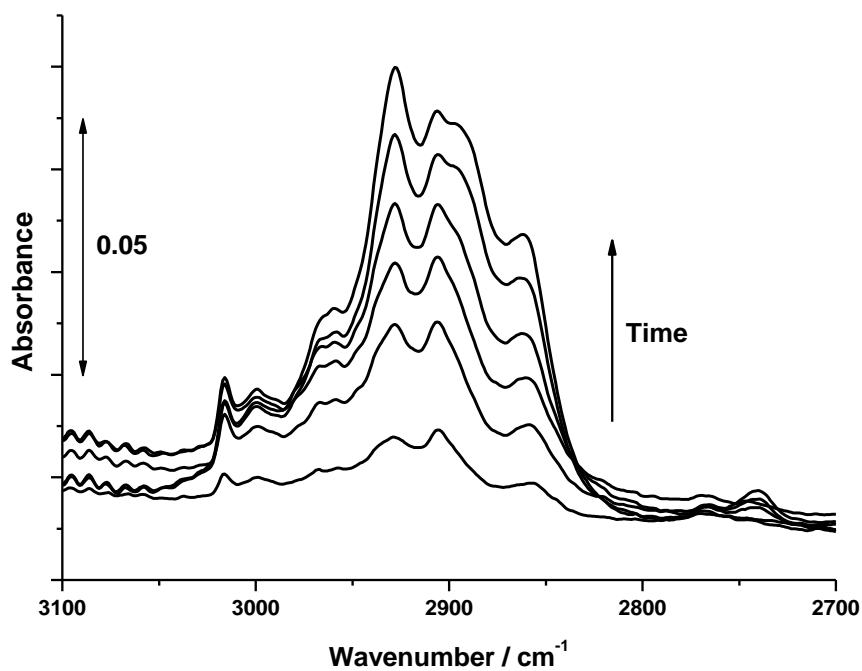


Figure 5: Selection of FTIR difference spectra for hydrocarbon region collected for a “separate disc” experiment under FT conditions (225°C, 10 bar, H<sub>2</sub>/CO = 2:1).

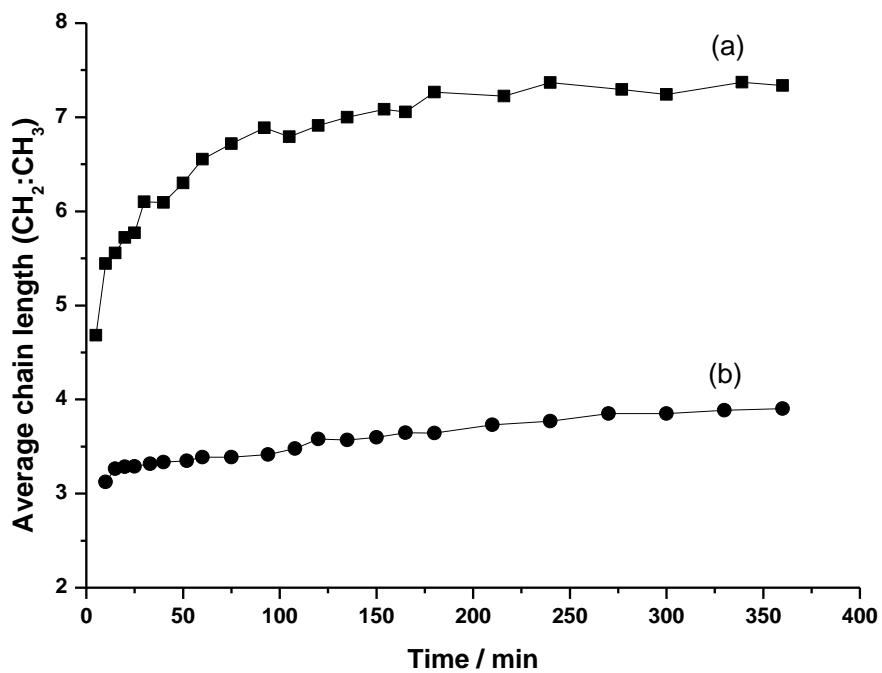
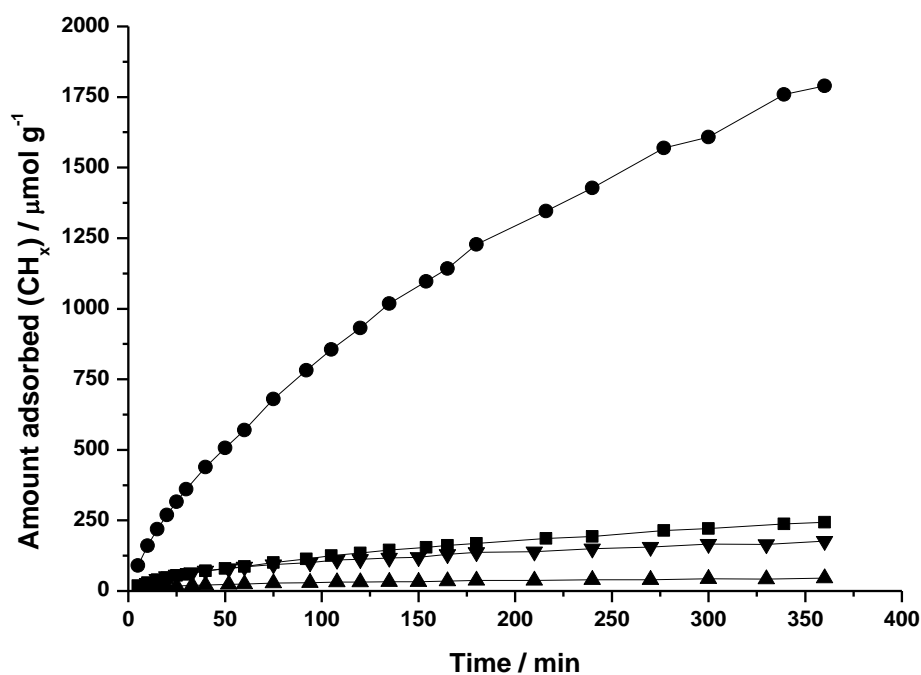
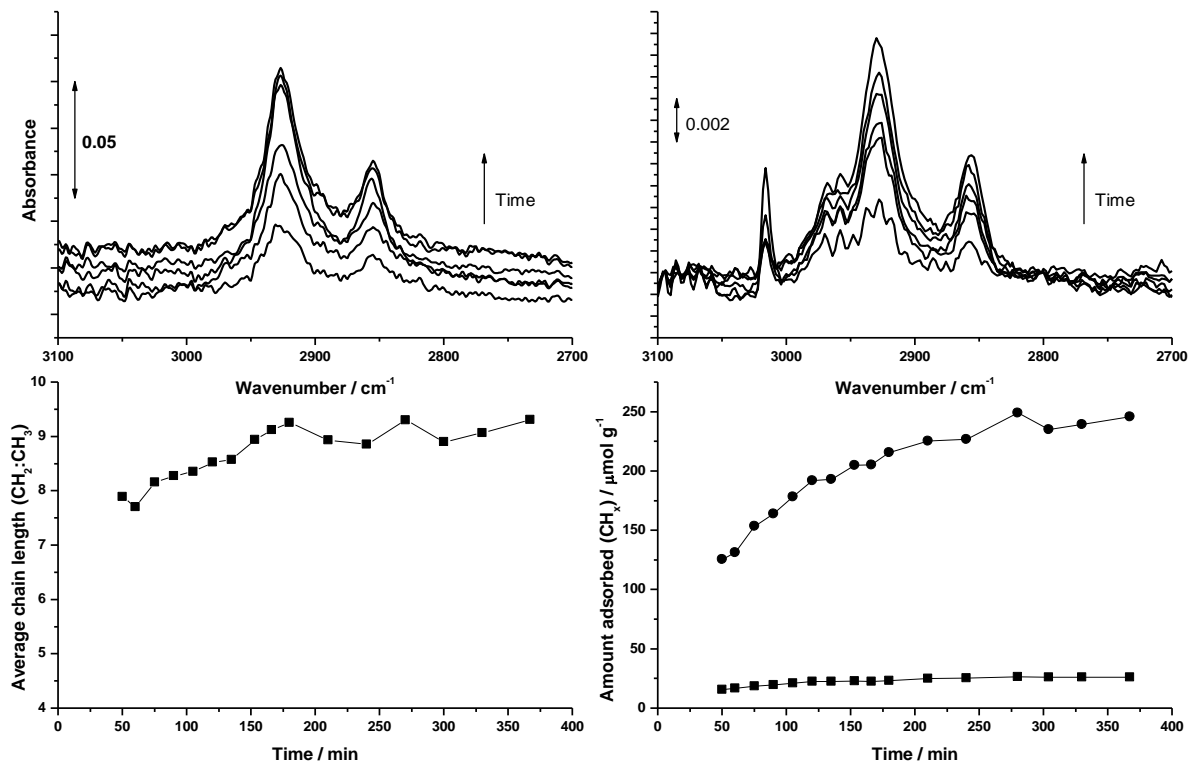


Figure 6: Estimation of chain lengths for hydrocarbon species detected for (a) a Co/Al<sub>2</sub>O<sub>3</sub> catalyst and (b) a separate disc of alumina under FT conditions (225°C, 10 bar, H<sub>2</sub>/CO = 2:1) using Equation 1.



**Figure 7:** Estimation of the total amount of hydrocarbon adsorbed in  $\mu\text{mol g}^{-1}$  of  $\text{CH}_x$  adsorbed to surface calculated using Equation 5 – Squares:  $\text{CH}_3$  on  $\text{Co}/\text{Al}_2\text{O}_3$ , circles:  $\text{CH}_2$  on  $\text{Co}/\text{Al}_2\text{O}_3$ , triangles:  $\text{CH}_3$  on  $\gamma$ -alumina, upside down triangle:  $\text{CH}_2$  on  $\gamma$ -alumina.



**Figure 8:** Selection of FTIR difference spectra for hydrocarbon region collected for, top left, a  $\text{Co}/\text{SiO}_2$  catalyst and top right, a separate disc of  $\text{SiO}_2$  under FT conditions ( $225^\circ\text{C}$ ,  $\text{H}_2/\text{CO} = 2:1$ , 10 bar for left hand spectra, 5 bar for right hand)

spectra). Bottom left: estimation of average length of hydrocarbons on a Co/SiO<sub>2</sub> catalyst determined using Equation 1. Bottom right: amount of CH<sub>x</sub> adsorbed to Co/SiO<sub>2</sub> surface calculated using Equation 5 – squares: CH<sub>3</sub>, circles: CH<sub>2</sub>.

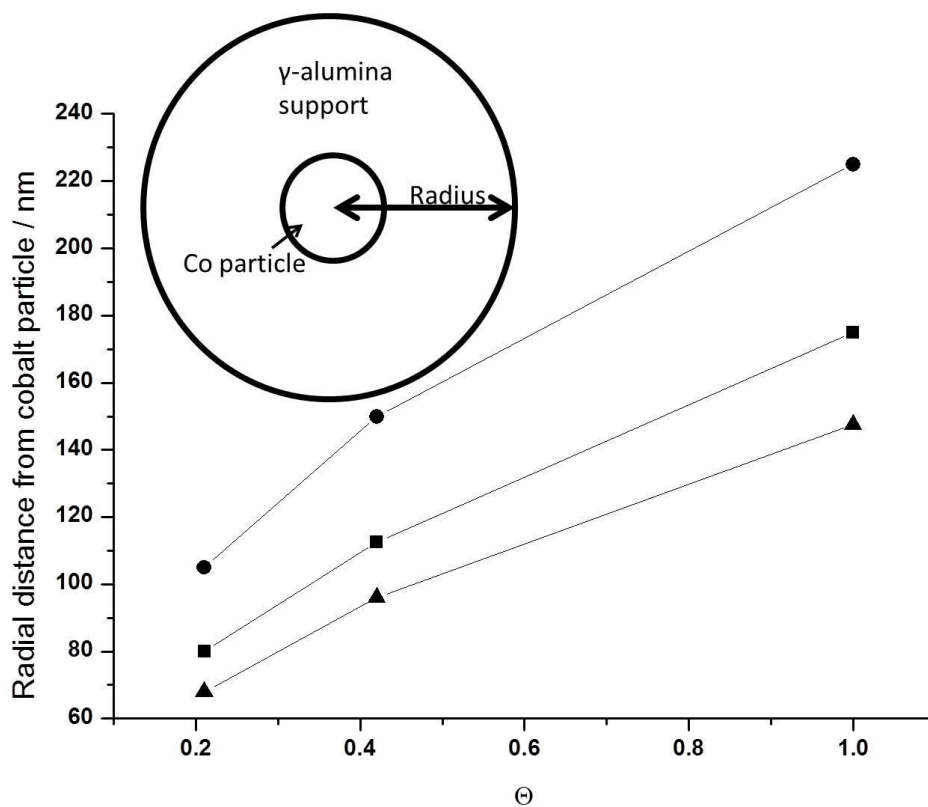


**Figure 9:** Coverage,  $\theta$ , versus radial distance (nm) from cobalt particle based on distance required for CH<sub>3</sub>:OH ratio of 1 to be attained. OH concentrations – circles: 4.9 OH nm<sup>-2</sup>, squares: 8.0 OH nm<sup>-2</sup>, triangles: 12.0 OH nm<sup>-2</sup>.